



Microbial life in the nascent Chicxulub crater

Bettina Schaefer¹, Kliti Grice^{1*}, Marco J.L. Coolen¹, Roger E. Summons², Xingqian Cui², Thorsten Bauersachs³, Lorenz Schwark^{1,3}, Michael E. Böttcher^{4,5,6}, Timothy J. Bralower⁷, Shelby L. Lyons⁷, Katherine H. Freeman⁷, Charles S. Cockell⁸, Sean P.S. Gulick⁹, Joanna V. Morgan¹⁰, Michael T. Whalen¹¹, Christopher M. Lowery⁹ and Vivi Vajda¹²

¹Western Australian Organic and Isotope Geochemistry Centre, School of Earth and Planetary Sciences, Curtin University, Perth, WA 6102, Australia

²Department of Earth, Atmospheric and Planetary Sciences, Massachusetts Institute of Technology, Cambridge, Massachusetts 02139, USA

³Organic Geochemistry Unit, Institute of Geosciences, Christian-Albrechts-University, Kiel 24118, Germany

⁴Geochemistry & Isotope Biogeochemistry Group, Department of Marine Geology, Leibniz Institute for Baltic Sea Research, 18119 Warnemünde, Germany

⁵Marine Geochemistry, University of Greifswald, 17489 Greifswald, Germany

⁶Department of Maritime Systems, Interdisciplinary Faculty, University of Rostock, 18059 Rostock, Germany

⁷Department of Geosciences, Pennsylvania State University, University Park, Pennsylvania 16802, USA

⁸School of Physics and Astronomy, University of Edinburgh, Edinburgh EH9 3FD, UK

⁹Institute for Geophysics, Jackson School of Geosciences, University of Texas at Austin, Austin, Texas 78712, USA

¹⁰Department of Earth Sciences and Engineering, Imperial College, London, London SW7 2AZ, UK

¹¹Department of Geosciences, University of Alaska, Fairbanks, Alaska 99775, USA

¹²Department of Palaeobiology, Swedish Museum of Natural History, P.O. Box 50007, Stockholm, Sweden

ABSTRACT

The Chicxulub crater was formed by an asteroid impact at ca. 66 Ma. The impact is considered to have contributed to the end-Cretaceous mass extinction and reduced productivity in the world's oceans due to a transient cessation of photosynthesis. Here, biomarker profiles extracted from crater core material reveal exceptional insights into the post-impact upheaval and rapid recovery of microbial life. In the immediate hours to days after the impact, ocean resurge flooded the crater and a subsequent tsunami delivered debris from the surrounding carbonate ramp. Deposited material, including biomarkers diagnostic for land plants, cyanobacteria, and photosynthetic sulfur bacteria, appears to have been mobilized by wave energy from coastal microbial mats. As that energy subsided, days to months later, blooms of unicellular cyanobacteria were fueled by terrigenous nutrients. Approximately 200 k.y. later, the nutrient supply waned and the basin returned to oligotrophic conditions, as evident from N₂-fixing cyanobacteria biomarkers. At 1 m.y. after impact, the abundance of photosynthetic sulfur bacteria supported the development of water-column photic zone euxinia within the crater.

INTRODUCTION

The impact crater at Chicxulub (Yucatán Peninsula, México) is the only terrestrial crater on Earth with a well-preserved peak ring (Hildebrand et al., 1991; Schulte et al., 2010; Morgan et al., 2016; Kring et al., 2017; Gulick et al., 2019). The asteroid impact is linked to the end-Cretaceous mass extinction event,

which wiped out 76% of all species worldwide (Sepkoski, 1996), along with a near-global loss of vegetation (Kring, 2007; Vajda and Bercovicci, 2014; Brugger et al., 2017). A collapse in phytoplankton productivity in the world's oceans (Hsü et al., 1982; Zachos and Arthur, 1986; Sepúlveda et al., 2009) occurred due to the sudden decline in photosynthesis as atmospheric particulates lowered light levels for years after the impact (Bardeen et al., 2017). In 2016, the peak ring of the Chicxulub crater

was cored (Fig. 1) by the International Ocean Discovery Program (IODP) and International Continental Scientific Drilling Program Expedition 364 (see the GSA Data Repository¹). A 130-m-thick interval of impact melt rock and upward-fining suevite, which overlies fractured basement rock, was deposited immediately after impact. The lower suevite, rich in impact melt rock, is directly overlain by material transported via ocean resurge and then by seiches and a tsunami deposit (Grice et al., 2009; Gulick et al., 2019; Osinski et al., 2019; Whalen, 2019, personal commun.). The overlying 0.75-m-thick, fine-grained, brown micritic limestone ("transitional unit"), deposited in days to years after the impact by continuing seiches and tsunami, contains microfossils of calcareous plankton and trace fossils of burrowing organisms (Whalen et al., 2017; Lowery et al., 2018; Gulick et al., 2019). The transitional unit is overlain by a thin green marlstone, followed by the deposition of "white" micritic limestone (616.55–616.24 m below seafloor [mbfs] within 30–200 k.y., representing the base of the succeeding pelagic-hemipelagic limestone deposit. Data to support the geology and relative timing of

*E-mail: K.Grice@curtin.edu.au

¹GSA Data Repository item 2020087, sample location and description, laboratory and analytical techniques, Figures DR1–DR4 (chromatograms), Figure DR5 (maturity parameters), Figure DR6 (fractional abundance of heterocyst glycolipids), and Figure DR7 (long-chain alkanes versus TOC), is available online at <http://www.geosociety.org/databaserepository/2020/>, or on request from editing@geosociety.org.

CITATION: Schaefer, B., et al., 2020, Microbial life in the nascent Chicxulub crater: *Geology*, v. 48, p. 328–332, <https://doi.org/10.1130/G46799.1>



Figure 1. Map showing International Ocean Discovery Program (IODP) Site M0077A (21.45°N, 89.95°W) at the Chicxulub crater, Mexico.

these events have been published by Gulick et al. (2019) and Lowery et al. (2018).

Evidence of ancient life is generally preserved in sediments as morphological fossils, trace fossils, and molecular fossils (biomarkers). Biomarkers are often well preserved in sediments even where visible mineralized fossils are absent, representing valuable signs of past life, especially microbial life. For example, in the Fiskeler Member in the end-Cretaceous boundary layer at Kulstirenden, Denmark, biomarkers showed that marine productivity recovered within a century following the Chicxulub impact (Sepúlveda et al., 2009). Here, we present biomarker distributions and sulfur isotopes of pyrite between 619 mbsf and 608 mbsf at IODP Site M0077A (21.45°N,

89.95°W). Our aim was to use biomarkers to reconstruct the origin, recovery, and development of microbial life and to determine the paleoenvironmental conditions in the crater from the time of impact to up to ~4 m.y. after the impact (Figs. 2 and 3).

MATERIALS AND METHODS

Detailed materials and methods are provided in the Data Repository. Briefly, samples were Soxhlet extracted, and the extracts were separated into apolar and polar fractions and analyzed by gas chromatography–mass spectrometry (GC-MS), metastable reaction monitoring (MRM), and high-performance liquid chromatography–tandem mass spectrometry (HPLC-MS²). The $\delta^{13}\text{C}$ and $\delta^{34}\text{S}$ values were measured on extracted residues. Total organic carbon (TOC) was determined by an elemental analyzer. Typical traces of GC-MS and MRM for procedural blanks and samples are given in Figures DR1–DR4 in the Data Repository.

RESULTS AND DISCUSSION

The TOC content (Fig. 2A) in the entire interval was low (0.06–0.2 wt%), consistent with carbonate dilution (see the Data Repository). The homohopane ratios [i.e., 22S/(22S + 22R)], were ≤ 0.6 , supporting a low thermal maturity through the section (see Fig. DR5; Peters et al., 2005). Despite low organic matter content and low abundances of biomarkers (Figs. 2 and 3), the record provided insights into the evolution of microbial communities in this exotic habitat.

First Days After Impact (619.31–617.33 mbsf)

The uppermost suevite was deposited by a tsunami within the first day after impact (Gulick et al., 2019). This tsunami transported reworked organic matter from outside the crater, as evidenced by the abundance and distribution of perylene and charcoal (Grice et al., 2009; Gulick et al., 2019). Reworked marine inputs shown by biomarkers included dominant $n\text{-C}_{17}/n\text{-C}_{19}$ alkanes, indicative of algae or cyanophytes (Fig. 2G). Further, abundant C₂₉ steranes from green algae and/or land plants (Fig. 2F) reflect a mixture of marine and terrigenous inputs. This interval also contains biomarkers derived from anoxygenic photosynthetic sulfur bacteria (i.e., isorenieratane, β -isorenieratane, and traces of chlorobactane and okenane; Summons and Powell, 1987; Brocks et al., 2005; Grice et al., 2005, 1996; Figs. 3B–3D). In addition, cyanobacterial biomarkers in the form of 2 α -methylhopanes (2 α -MeH; Summons et al., 1999; Welander et al., 2010) and heterocyst glycolipids (HGs) were observed. The latter, diagnostic for N₂-fixing cyanobacteria, represent the oldest reported intact HGs (Fig. 2D; Bauersachs et al., 2010). From the presence of terrestrial signatures and the depositional regime, we infer that all the organic signatures are reworked materials, likely derived from carbonate platforms and coastal environments close to the site. The biomarkers listed above were also identified in overlying sediments (617.33–608.48 mbsf), where they represent organisms living within the nascent crater. Here, we evaluate the oceanographic and redox conditions in the impact basin as inferred from the biological origins of these compounds.

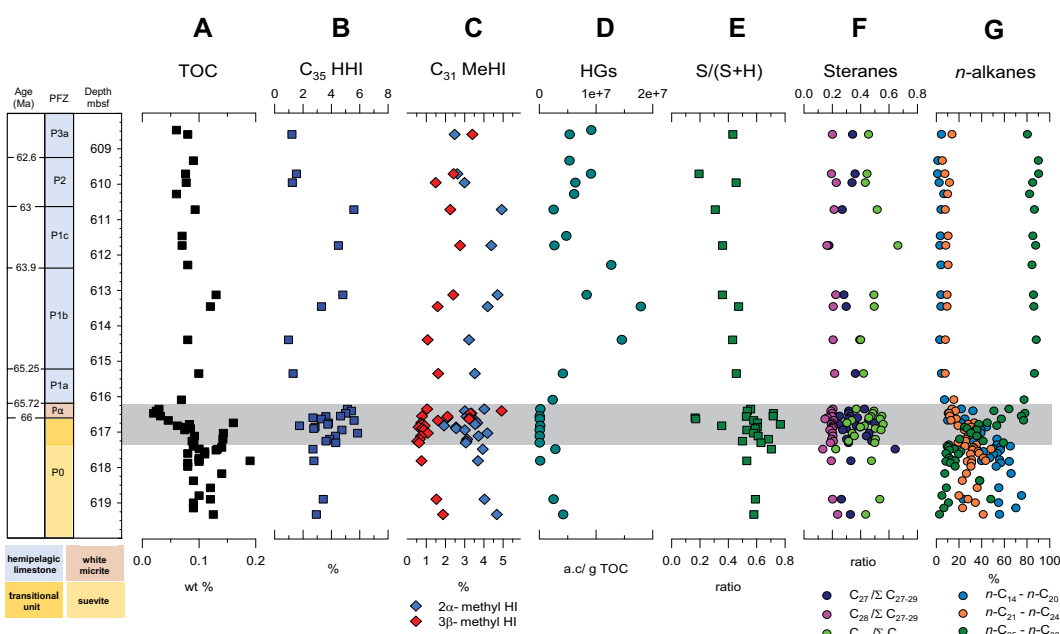
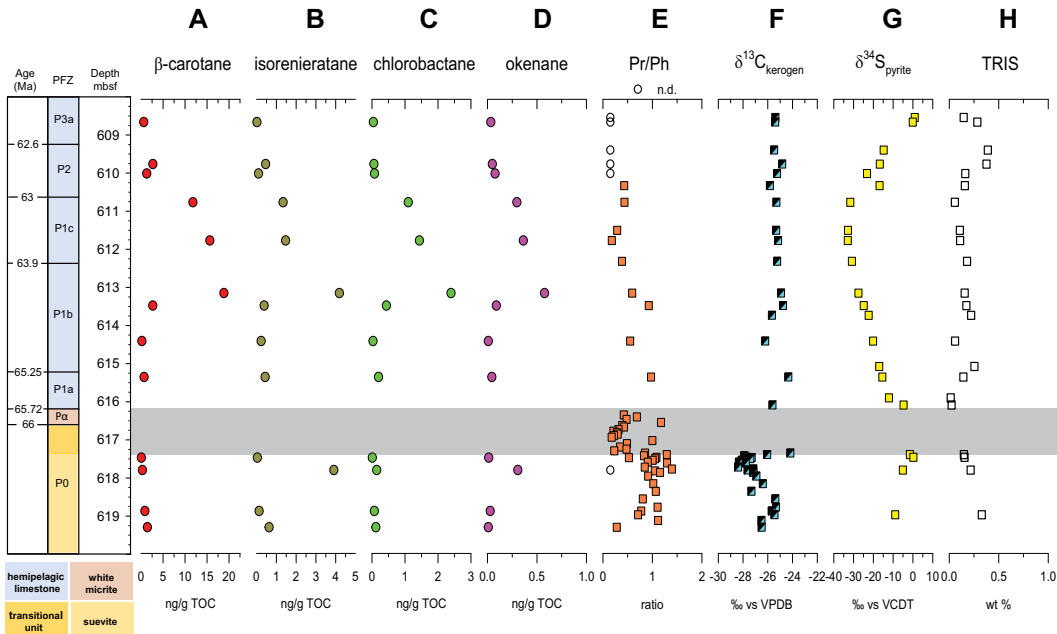


Figure 2. Composite plot of biomarker data in extracted bitumen samples against the lithology of the Chicxulub core (Yucatán Peninsula, México) from International Ocean Discovery Program (IODP) Site M0077A. Compounds were identified by comparison with standard components (see the Data Repository [see footnote 1] for analyses). Total organic carbon (TOC) content in entire interval was very low (0.2 wt%). C₃₅ homohopane index (bacterial activity), 2 α -methyl (cyanobacteria) and 3 β -methyl (methanotrophs) hopanes, and heterocysts glycolipids (HGs), which are indicative of N₂-fixing cyanobacteria. Sterane index, S/(S + H), is indicative of relative inputs of eukaryotic (algae and higher plants) and bacterial sources. C₂₇–C₂₉ steranes (algae, land plants, and fungi) and n-C₂₅ to n-C₃₃ waxes from land plants are prevalent compared to low-molecular-weight n-alkanes.

Biostratigraphy was used for age determination (Gradstein et al., 2012; Lowery et al., 2018). PFZ—planktic foraminifer zone; HHI—homohopane index; MeHI—Methylhopane index. (A) TOC concentrations (wt%). (B) C₃₅ HHI ($[\text{C}_{35} \alpha/\beta \text{S} + \text{R}/\sum_{\text{C}_{31-35}} \alpha/\beta \text{S} + \text{R}] \times 100$). (C) Methylhopane indices (e.g., $[\text{C}_{31} 2\alpha\text{-methyl}/(\text{C}_{30}\alpha\beta + \text{C}_{31} 2\alpha\text{-methyl})] \times 100$). (D) HG abundance (area counts/g of TOC). (E) Sterane/sterane + hopane ratio ($\text{C}_{27-29} \text{ steranes}/(\text{C}_{27-29} \text{ steranes} + \text{C}_{30-35} \text{ hopanes})$). (F) Steranes ($\text{C}_{27}/\sum \text{C}_{27-29}$, $\text{C}_{28}/\sum \text{C}_{27-29}$, $\text{C}_{29}/\sum \text{C}_{27-29}$). (G) n-alkanes ($n\text{-C}_{14}-n\text{-C}_{33}$).



determination (Gradstein et al., 2012; Lowery et al., 2018). PFZ—planktic foraminifer zones; TOC—total organic carbon. (A) β -carotane concentrations (ng/g TOC). (B) Isorenieratane concentrations (ng/g TOC). (C) Chlorobactane concentrations (ng/g TOC). (D) Okenane concentrations (ng/g TOC). (E) Pristane/phytane (Pr/Ph) ratio. (F) $\delta^{13}\text{C}_{\text{kerogen}}$ values (‰, relative to Vienna PeeDee belemnite [VPDB]). (G) $\delta^{34}\text{S}_{\text{pyrite}}$ values (‰, relative to Vienna Canyon Diablo Troilite [VCDT]). (H) Total reduced inorganic sulfur (TRIS) concentrations (wt%).

Recovery—The First 200 k.y. (617.33–616.24 mbsf)

The interval deposited immediately after impact is represented by the transitional unit (617.33–616.58 mbsf) of fine-grained brown micrite and overlying green marlstone, and it is likely to contain the first record of microbial life after the impact (Lowery et al., 2018; Bralower, 2019, personal commun.). The succeeding “white micrite” is possibly a result of calcite formed photosynthetically by cyanobacteria that replaced the calcareous nanoplankton and other algae across the Cretaceous–Paleogene boundary (Bralower, 2019, personal commun.).

Our study provides the first evidence of cyanobacteria 30 k.y. after impact at 617.33–616.58 mbsf, from abundant C₃₁₊ hopanes (Figs. 2B and 2C; Rohmer et al., 1984; Summons et al., 1999; Brocks, 2018). The 2 α -MeH ratios (1.9 and 4.2; Fig. 2C), in agreement with those reported for the Fiskeler Member boundary layer, are typical of marine conditions (Sepúlveda et al., 2009). However, the ratios observed here are significantly lower than those reported in Permian-Triassic (Cao et al., 2009) and Triassic-Jurassic (Kasprak et al., 2015) boundary sections.

The sterane/(sterane + hopane) ratios [S/(S + H)] were found to be low (0.17 and 0.7; Fig. 2E), showing low algal inputs relative to bacteria, particularly cyanobacteria (Brocks, 2018). In the Fiskeler Member boundary layer, the lowest S/(S + H) ratio was assigned to a decreased algal input, followed by an immediate increase, suggesting a rapid resurgence of algae when solar irradiance returned to pre-impact lev-

els (Sepúlveda et al., 2009). In the transitional unit, the S/(S + H) ratio changed within multiple intervals, suggesting that the organic matter in the crater was a mixture of transported and autochthonous material, distinct from other Cretaceous–Paleogene sites (Sepúlveda et al., 2009). A similar trend was observed in the 2 α -MeH index and the homohopane index (HHI) (Figs. 2B, 2C, and 2E). The HHI (5.8) and 2 α -MeH index (4.2) are consistent with anoxic-euxinic conditions (Sepúlveda et al., 2009; Hamilton et al., 2017), which are also reflected by the low pristane/phytane ratios (Figs. 2B, 2C, and 3E). The HHI is based on the increased preservation of extended hopanes (>C₃₃) under euxinic conditions (Peters and Moldowan, 1991) through reduction and cross-linking with reduced sulfur species (Köster et al., 1997). The shifts in high to low S/(S + H) ratios suggest that sedimentation was influenced by water movement, most likely seiches (Gulick et al., 2019) and resuspension (Lowery et al., 2018).

The HGs were observed to be low in abundance (Fig. 2D) in this interval, and exclusively consisted of the HG₂₆ diol and HG₂₆ keto-ol (Fig. DR6), identified in coastal microbial mats (Bauersachs et al., 2011), brackish-marine environments (Sollai et al., 2017), and in axenic cultures of nostocalean cyanobacteria such as *Anabaena* spp. or *Nodularia* spp. (Bauersachs et al., 2009, 2017). HG₂₈ triols have been reported in free-living marine cyanobacteria (Bale et al., 2018). It is therefore plausible that the HG₂₆ diol and HG₂₆ keto-ol are also derived from a marine source. The low abundance of both components, however, suggests only low

Figure 3. Composite plot of biomarker data in bitumen samples against the lithology of the Chicxulub core (Yucatán Peninsula, Mexico) from International Ocean Discovery Program (IODP) Site M0077A. Compounds were identified by comparison with standard components (see the Data Repository [see footnote 1] for analyses). Relatively high abundances of β -carotane and Chlorobiaceae biomarkers were observed in the hemipelagic limestone section (isorenieratane, chlorobactane, and okenane). There were no aromatic hydrocarbons available to conduct metastable reaction monitoring (MRM) analysis for interval 617.35–616.24 mbsf. Low ratios of pristane to phytane (<1) were observed, minimizing in the limestone interval, consistent with depleted values of $\delta^{34}\text{S}$ of pyrite and abundant total reduced inorganic sulfur (TRIS). Biostratigraphy was used for age

productivity of N₂-fixing heterocystous cyanobacteria in the first 200 k.y. after the impact. An increased influx of terrigenous nutrients would have helped to sustain phytoplankton, as shown by the paired increase in the abundance of long-chain waxy n-alkanes (C₂₅–C₃₃) and C₂₉ steranes (0.3–0.56; Figs. 2G and 2F) from plants and green algae (Eglinton and Hamilton, 1967; Volkman, 1986; Kodner et al., 2008). The 3 β -MeH index (Fig. 2C) showed an increase at the top of the transitional unit (616.62–616.58 mbsf) and in the white micrite, indicating the presence of methanotrophs (e.g., Ding and Valentine, 2008).

200 k.y. to 4 m.y. After Impact (616.24–608.48 mbsf)

A substantial shift in the microbial community was found in the middle and upper parts of the hemipelagic limestone horizon. The HG distribution patterns and abundances showed considerable changes indicating shifts in the cyanobacterial community and an increase in cyanobacterial productivity by two orders of magnitude (0.23×10^7 area counts/g TOC) compared to the transitional unit, with maximum concentrations at 613.45 mbsf (Fig. 2D; Fig. DR6).

In contrast, the 2 α -MeH index remained constant, with a slight increase at 613.45 mbsf, whereas the HHI increased again between 613.45 and 610.72 mbsf. This increase in (cyano)bacterial biomarkers and the concomitant rise in the abundance of N₂-fixing heterocystous cyanobacteria suggest a shift toward a nitrogen-limited environment, perhaps triggered by water column stratification. Another possibility is that

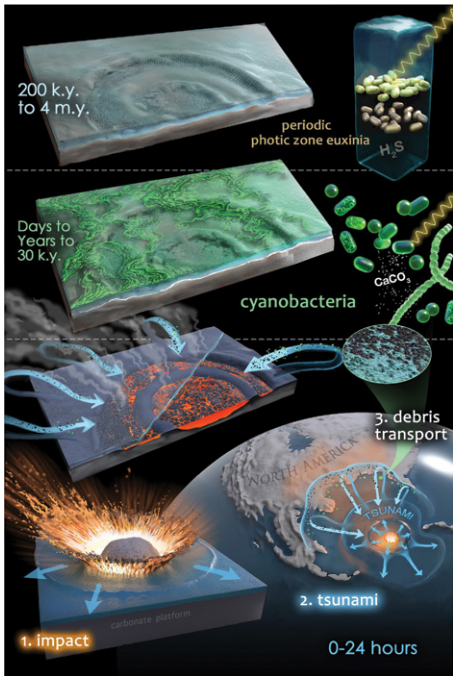


Figure 4. Evolution of microbial communities in the Chicxulub crater, Yucatán Peninsula, Mexico. Image by Victor Leshyk.

these organisms were allochthonous and were transported into the crater from microbial mats living in relatively shallow waters. The limestone interval between 613.45 and 610.72 mbsf (ca. 64.4–63.1 Ma) indeed indicated anoxic conditions during deposition, depicted by low pristane/phytane ratios (<1; Fig. 3E), abundant β -carotane from autotrophs, and highly characteristic photic zone euxinia (PZE) biomarkers from green-green and brown-green pigmented Chlorobiaceae (e.g., chlorobactane and isorenieratane), and purple pigmented Chromatiaceae (okenane; Figs. 3A–3D; Imhoff, 2004). Chlorobiaceae and Chromatiaceae are anaerobic photoautotrophs that use hydrogen sulfide (generated by sulfate-reducing bacteria) as an electron donor and biosynthesize specific bacteriochlorophyll and accessory carotenoid pigments to capture longer wavelengths of light energy to fix CO_2 (Pfennig, 1978). Such organisms flourish in benthic mats and as plankton concentrated at the chemocline of lakes or restricted marine basins where sulfide concentrations are high within the photic zone; hence, they are indicative of PZE conditions (Pfennig, 1978; Grice et al., 2005; French et al., 2015). In this limestone interval, total reduced inorganic sulfur was abundant, with $\delta^{34}\text{S}$ values ranging from $\sim -22\text{\textperthousand}$ at 613.71 mbsf to $\sim -33\text{\textperthousand}$ at ~ 611 mbsf, consistent with nonlimiting sulfate concentrations, water-column PZE (Figs. 3G and 3H), and enhanced pyrite burial (Fig. 3H; Lyons, 1997; Böttcher and Lepland, 2000). Similar $\delta^{34}\text{S}$ values have been reported for reduced sulfur in Cretaceous black shales (Hetzel et al., 2006; Witts et al.,

2018). Diagenetic pyrite in shell fillings and sediment matrix indicates recrystallization of primary frambooids. The pronounced $\delta^{34}\text{S}$ depletion compared to the estimated value of contemporaneous seawater ($15\text{\textperthousand}$ – $20\text{\textperthousand}$; Strauss, 1997; Witts et al., 2018) signifies that microbial sulfate reduction probably took place in the water column (Figs. 3G and 3H; Strauss, 1997).

Associated with compelling indicators that periodic PZE was prevalent in the Chicxulub crater from ca. 64.4 Ma to 63.1 Ma, the molecular evidence indicates that oxygenated waters overlay the anoxic and sulfidic interval of the water column (Figs. 2B–2D, 3E, 3G, and 3H). During this time interval, methane from anoxic sediments underlying a sulfidic water column likely migrated upward until it was oxidized by microaerophilic methanotrophic bacteria at the chemocline, as evidenced by 3β -MeHI (Fig. 2C). An alternative scenario is the possibility of an oxygen minimum zone (OMZ) existing in the crater water.

CONCLUSIONS

The evolution of microbial communities in the Chicxulub crater was investigated using molecular and isotopic signatures, as summarized in Figure 4. We propose a scenario where, in the initial days after the asteroid impact, debris from microbial mats containing N_2 -fixing heterocystous cyanobacteria and photosynthetic sulfur bacteria was eroded from adjacent carbonate platforms and transported by ocean resurge or tsunamis into the crater. Microbial ecosystem communities were in a constant state of dynamic flux during the early evolution of the crater. Diminution of sunlight following the impact led to a dramatic decline in cyanobacterial productivity in the crater waters. However, rapid recovery of phytoplankton occurred in the first 200 k.y., and marine primary production was fueled by an influx of terrigenous nutrients. Phytoplankton communities continued to experience rapid changes over the following 4 m.y. The nascent Chicxulub crater basin was accompanied by major transitions in nutrient and oxygen supplies (periods of euxinia) that shaped the recovery of microbial life.

ACKNOWLEDGMENTS

The research used samples and data provided by the International Ocean Discovery Program (IODP). Expedition 364 was implemented by the European Consortium for Ocean Research Drilling (ECORD) and jointly funded by the IODP and the International Continental Scientific Drilling Program (ICDP), with contributions and logistical support from the Yucatan State Government and Universidad Nacional Autónoma de México (UNAM). We thank Peter Hopper and Alex Holman for their technical support with GC-MS analyses, and Iris Schmiedinger for isotope mass spectrometric analysis. Grice, Coolen, and Summons thank the Australian Research Council (ARC) for an ARC Discovery grant (DP180100982) titled “The recovery of life recorded at the end-Cretaceous impact crater.” Schaefer thanks Curtin University for an Australian postgraduate award. Coolen and Grice thank IODP and Australian and New Zealand

legacy IODP funding (364 postcruise funding, 2016–2018) of “The Chicxulub post-impact crater record: Duration of a giant hydrothermal system and window into the resurgence and evolution of marine and terrestrial life” project. Schwark and Bauersachs received support via Deutsche Forschungsgemeinschaft grant Schw554/26. Freeman and Bralower, Gulick and Lowery, and Whalen were supported by U.S. National Science Foundation grants OCE 1736951, 1737351, and 1737199, respectively. Joanna Morgan was supported by UK NERC grant NE/P005217/1. Thanks go to Julio Sepúlveda for helpful comments on an earlier version of this manuscript. We thank the anonymous reviewers for their constructive comments, which helped to improve this manuscript. This is University of Texas Institute for Geophysics Contribution #3529.

REFERENCES CITED

- Bale, N.J., Hopmans, E.C., Dorhout, D., Stal, L.J., Grego, M., van Bleijswijk, J., Sinninghe Damsté, J.S., and Schouten, S., 2018, A novel heterocyst glycolipid detected in a pelagic N_2 -fixing cyanobacterium of the genus *Calothrix*: Organic Geochemistry, v. 123, p. 44–47, <https://doi.org/10.1016/j.orggeochem.2018.06.009>.
- Bardeen, C.G., Garcia, R.R., Toon, O.B., and Conley, A.J., 2017, On transient climate change at the Cretaceous-Paleogene boundary due to atmospheric soot injections: Proceedings of the National Academy of Sciences of the United States of America, v. 114, p. E7415–E7424, <https://doi.org/10.1073/pnas.1708980114>.
- Bauersachs, T., Compaoré, J., Hopmans, E.C., Stal, L.J., Schouten, S., and Sinninghe Damsté, J.S., 2009, Distribution of heterocyst glycolipids in cyanobacteria: Phytochemistry, v. 70, p. 2034–2039, <https://doi.org/10.1016/j.phytochem.2009.08.014>.
- Bauersachs, T., Speelman, E.N., Hopmans, E.C., Reichart, G.J., Schouten, S., and Sinninghe Damsté, J.S., 2010, Fossilized glycolipids reveal past oceanic N_2 fixation by heterocystous cyanobacteria: Proceedings of the National Academy of Sciences of the United States of America, v. 107, p. 190–194, <https://doi.org/10.1073/pnas.1007526107>.
- Bauersachs, T., Compaoré, J., Severin, E., Hopmans, E.C., Stal, L.J., Schouten, S., and Sinninghe Damsté, J.S., 2011, Diazotrophic microbial community of coastal microbial mats of the southern North Sea: Geobiology, v. 9, p. 349–359, <https://doi.org/10.1111/j.1472-4669.2011.00280.x>.
- Bauersachs, T., Talbot, H.M., Sidgwick, F., Sivonen, K., and Schwark, L., 2017, Lipid biomarker signatures as tracers for harmful cyanobacterial blooms in the Baltic Sea: PLoS One, v. 12, e0186360, <https://doi.org/10.1371/journal.pone.0186360>.
- Böttcher, M.E., and Lepland, A., 2000, Biogeochemistry of sulfur in a sediment core from the west-central Baltic Sea: Evidence from stable isotopes and pyrite textures: Journal of Marine Systems, v. 25, p. 299–312, [https://doi.org/10.1016/S0924-7963\(00\)00023-3](https://doi.org/10.1016/S0924-7963(00)00023-3).
- Brocks, J.J., 2018, The transition from a cyanobacterial to algal world and the emergence of animals: Emerging Topics in Life Sciences, v. 2, p. 181–190, <https://doi.org/10.1042/ETLS20180039>.
- Brocks, J.J., Love, D., Summons, R.E., Knoll, A.H., Logan, G.A., and Bowden, S.A., 2005, Biomarker evidence for green and purple sulphur bacteria in a stratified Palaeoproterozoic sea: Nature, v. 437, p. 866–870, <https://doi.org/10.1038/nature04068>.
- Brugger, J., Feulner, G., and Petri, S., 2017, Baby, it’s cold outside: Climate model simulations of the effects of the asteroid impact at

- the end of the Cretaceous: *Geophysical Research Letters*, v. 44, p. 419–427, <https://doi.org/10.1002/2016GL072241>.
- Cao, C., Love, G.D., Hays, L.E., Wang, W., Shen, S., and Summons, R.E., 2009, Biogeochemical evidence for euxinic oceans and ecological disturbance presaging the end-Permian mass extinction event: *Earth and Planetary Science Letters*, v. 281, p. 188–201, <https://doi.org/10.1016/j.epsl.2009.02.012>.
- Ding, H., and Valentine, D.L., 2008, Methanotrophic bacteria occupy benthic microbial mats in shallow marine hydrocarbon seeps, Coal Oil Point, California: *Journal of Geophysical Research-Biogeosciences*, v. 113, G01015, <https://doi.org/10.1029/2007JG000537>.
- Eglinton, G., and Hamilton, R.J., 1967, Leaf epicuticular waxes: *Science*, v. 156, p. 1322–1335, <https://doi.org/10.1126/science.156.3780.1322>.
- French, K.L., Rocher, D., Zumberge, J.E., and Summons, R.E., 2015, Assessing the distribution of sedimentary C₄₀ carotenoids through time: *Geobiology*, v. 13, p. 139–151, <https://doi.org/10.1111/gbi.12126>.
- Gradstein, F.M., Ogg, J.G., Schmitz, M., and Ogg, G., eds., 2012, *The Geologic Time Scale 2012*: Amsterdam, Elsevier, 1176 p., <https://doi.org/10.1127/0078-0421/2012/0020>.
- Grice, K., Schaeffer, P., Schwark, L., and Maxwell, J.R., 1996, Molecular indicators of palaeoenvironmental conditions in an immature Permian shale (Kupferschiefer, Lower Rhine Basin, northwest Germany) from free and S-bound lipids: *Organic Geochemistry*, v. 25, p. 131–147, [https://doi.org/10.1016/S0146-6380\(96\)00130-1](https://doi.org/10.1016/S0146-6380(96)00130-1).
- Grice, K., Cao, C., Love, C.D., Böttcher, M.E., Twitchett, R.J., Grosjean, E., Summons, R.E., Turgeon, S.C., Dunning, W., and Jin, Y., 2005, Photic zone euxinia during the Permian-Triassic superoxic event: *Science*, v. 307, p. 706–709, <https://doi.org/10.1126/science.1104323>.
- Grice, K., Lu, H., Atahan, P., Asif, M., Hallmann, C., Greenwood, P., Maslen, E., Tulipani, S., Williford, K., and Dodson, J., 2009, New insights into the origin of perylene in geological samples: *Geochimica et Cosmochimica Acta*, v. 73, p. 6531–6543, <https://doi.org/10.1016/j.gca.2009.07.029>.
- Gulick, S., et al., 2019, First days of the Cenozoic: *Proceedings of the National Academy of Sciences of the United States of America*, v. 116, p. 19342–19351, <https://doi.org/10.1073/pnas.1909479116>.
- Hamilton, T.L., Welander, P.V., Albrecht, H.L., Fulton, J.M., Schaperdoth, I., Bird, L.R., Summons, R.E., Freeman, K.H., and Macalady, J.L., 2017, Microbial communities and organic biomarkers in a Proterozoic-analog sinkhole: *Geobiology*, v. 15, p. 784–797, <https://doi.org/10.1111/gbi.12252>.
- Hetzell, A., Brumsack, H.-J., Schnetger, B., and Böttcher, M.E., 2006, Inorganic geochemical characterization of lithologic units recovered during ODP Leg 207 (Demerara Rise), in Mosher, D.C., Erbacher, J., and Malone, M.J., eds., *Ocean Drilling Program, Scientific Results Volume 207*: College Station, Texas, Ocean Drilling Program, p. 1–37, <https://doi.org/10.2973/odp.proc sr.207.107.2006>.
- Hildebrand, A.R., et al., 1991, Chicxulub crater: A possible Cretaceous/Tertiary boundary impact crater on the Yucatan Peninsula, Mexico: *Geology*, v. 19, p. 867–871, [https://doi.org/10.1130/0091-7613\(1991\)019<867:CCAPCT>2.3.CO;2](https://doi.org/10.1130/0091-7613(1991)019<867:CCAPCT>2.3.CO;2).
- Hsü, K.J., et al., 1982, Mass mortality and its environmental and evolutionary consequences: *Science*, v. 216, p. 249–256, <https://doi.org/10.1126/science.216.4543.249>.
- Imhoff, J., 2004, Taxonomy and physiology of phototrophic purple bacteria and green sulfur bacteria, in Blankenship, R., Madigan, M., and Bauer, C., eds., *Anoxygenic Photosynthetic Bacteria*: Amsterdam, Springer Netherlands, p. 1–15, https://doi.org/10.1007/0-306-47954-0_1.
- Kasprak, A.H., Sepúlveda, J., Price-Waldman, R., Williford, K.H., Schoepfer, S.D., Haggart, J.W., Ward, P.D., Summons, R.E., and Whiteside, J.H., 2015, Episodic photic zone euxinia in the northeastern Panthalassic Ocean during the end-Triassic extinction: *Geology*, v. 43, p. 307–310, <https://doi.org/10.1130/G36371.1>.
- Kodner, R.B., Pearson, A., Summons, R.E., and Knoll, A.H., 2008, Sterols in red and green algae: Quantification, phylogeny, and relevance for the interpretation of geologic steranes: *Geobiology*, v. 6, p. 411–420, <https://doi.org/10.1111/j.1472-4669.2008.00167.x>.
- Köster, J., van Kaam-Peters, H.M.E., Koopmans, M.P., de Leeuw, J.W., and Sinninghe Damsté, J.S., 1997, Sulphurisation of homohopanoids: Effects on carbon number distribution, speciation, and 22S/22R epimer ratios: *Geochimica et Cosmochimica Acta*, v. 61, p. 2431–2452, [https://doi.org/10.1016/S0016-7037\(97\)00110-5](https://doi.org/10.1016/S0016-7037(97)00110-5).
- Kring, D.A., 2007, The Chicxulub impact event and its environmental consequences at the Cretaceous-Tertiary boundary: *Palaeogeography, Palaeoclimatology, Palaeoecology*, v. 255, p. 4–21, <https://doi.org/10.1016/j.palaeo.2007.02.037>.
- Kring, D.A., Claeys, P., Gulick, S.P.S., Morgan, J.V., and Collins, G.S., 2017, Chicxulub and the exploration of large peak-ring impact craters through scientific drilling: *GSA Today*, v. 27, no. 10, p. 4–8, <https://doi.org/10.1130/GSATG352A.1>.
- Lowery, C.M., et al., 2018, Rapid recovery of life at ground zero of the end-Cretaceous mass extinction: *Nature*, v. 558, p. 288–291, <https://doi.org/10.1038/s41586-018-0163-6>.
- Lyons, T.W., 1997, Sulfur isotopic trends and pathways of iron sulfide formation in upper Holocene sediments of the anoxic Black Sea: *Geochimica et Cosmochimica Acta*, v. 61, p. 3367–3382, [https://doi.org/10.1016/S0016-7037\(97\)00174-9](https://doi.org/10.1016/S0016-7037(97)00174-9).
- Morgan, J.V., et al., 2016, The formation of peak rings in large impact craters: *Science*, v. 354, p. 878–882, <https://doi.org/10.1126/science.1258030>.
- Osinski, G.R., Grieve, R.A., Hill, P.J., Simpson, S.L., Cockell, C., Christeson, G.L., Ebert, M., Gulick, S., Melosh, H.J., Riller, U., and Tikoo, S.M., 2019, Explosive interaction of impact melt and seawater following the Chicxulub impact event: *Geology*, v. 48, p. 108–112, <https://doi.org/10.1130/G46783.1>.
- Peters, K.E., and Moldowan, J.M., 1991, Effects of source, thermal maturity, and biodegradation on the distribution and isomerization of homohopanes in petroleum: *Organic Geochemistry*, v. 17, p. 47–61, [https://doi.org/10.1016/0146-6380\(91\)90039-M](https://doi.org/10.1016/0146-6380(91)90039-M).
- Peters, K.E., Walters, C.C., and Moldowan, J.M., 2005, *The Biomarker Guide: Volume 2: Biomarkers and Isotopes in Petroleum Exploration and Earth History* (2nd ed.): Cambridge, UK, Cambridge University Press, 700 p.
- Pfennig, N., 1978, General physiology and ecology of photosynthetic bacteria, in Clayton, R.K., and Sistrom, W.R., eds., *The Photosynthetic Bacteria*: New York, Plenum, p. 3–18.
- Rohmer, M., Bouvier-Nave, P., and Ourisson, G., 1984, Distribution of hopanoid triterpenes in prokaryotes: *Microbiology*, v. 130, p. 1137–1150, <https://doi.org/10.1099/00221287-130-5-1137>.
- Schulte, P., et al., 2010, The Chicxulub asteroid impact and mass extinction at the Cretaceous-Paleogene boundary: *Science*, v. 327, p. 1214–1218, <https://doi.org/10.1126/science.1177265>.
- Sepkoski, J.J., 1996, Patterns of Phanerozoic extinction: A perspective from global databases, in Walliser, O.H., ed., *Global Events and Event Stratigraphy in the Phanerozoic, Results of the International Interdisciplinary Cooperation in the IGCP-Project 216 “Global Biological Events in Earth History”*: Berlin, Springer, p. 35–51.
- Sepúlveda, J., Wendler, J.E., Summons, R.E., and Hinrichs, K.-U., 2009, Rapid resurgence of marine productivity after the Cretaceous-Paleogene mass extinction: *Science*, v. 326, p. 129–132, <https://doi.org/10.1126/science.1176233>.
- Sollai, M., Hopmans, E.C., Bale, N.J., Mets, A., Warden, L., Moros, M., and Sinninghe Damsté, J.S., 2017, The Holocene sedimentary record of cyanobacterial glycolipids in the Baltic Sea: An evaluation of their application as tracers of past nitrogen fixation: *Biogeosciences*, v. 14, p. 5789–5804, <https://doi.org/10.5194/bg-14-5789-2017>.
- Strauss, H., 1997, The isotopic composition of sedimentary sulfur through time: *Palaeogeography, Palaeoclimatology, Palaeoecology*, v. 132, p. 97–118, [https://doi.org/10.1016/S0031-0182\(97\)00067-9](https://doi.org/10.1016/S0031-0182(97)00067-9).
- Summons, R.E., and Powell, T.G., 1987, Identification of aryl isoprenoids in source rocks and crude oils: Biological markers for the green sulphur bacteria: *Geochimica et Cosmochimica Acta*, v. 51, p. 557–566, [https://doi.org/10.1016/0016-7037\(87\)90069-X](https://doi.org/10.1016/0016-7037(87)90069-X).
- Summons, R.E., Jahnke, L.L., Hope, J.M., and Logan, G.A., 1999, 2-methylhopanoids as biomarkers for cyanobacterial oxygenic photosynthesis: *Nature*, v. 400, p. 554–557, <https://doi.org/10.1038/23005>.
- Vajda, V., and Bercovici, A., 2014, The global vegetation pattern across the Cretaceous-Paleogene mass extinction interval: A template for other extinction events: *Global and Planetary Change*, v. 122, p. 29–49, <https://doi.org/10.1016/j.gloplacha.2014.07.014>.
- Volkman, J.K., 1986, A review of sterol markers for marine and terrigenous organic matter: *Organic Geochemistry*, v. 9, p. 83–99, [https://doi.org/10.1016/0146-6380\(86\)90089-6](https://doi.org/10.1016/0146-6380(86)90089-6).
- Welander, P.V., Coleman, M.L., Sessions, A.L., Summons, R.E., and Newman, D.K., 2010, Identification of a methylase required for 2-methylhopanoid production and implications for the interpretation of sedimentary hopanes: *Proceedings of the National Academy of Sciences of the United States of America*, v. 107, p. 8537–8542, <https://doi.org/10.1073/pnas.0912949107>.
- Whalen, M., et al., 2017, Sedimentologic and stable isotopic evidence for rapid post-impact sedimentation in the Chicxulub impact crater: *Geological Society of America Abstracts with Programs*, v. 49, no. 6, abstract 192-6, <https://doi.org/10.1130/abs/2017AM-299302>.
- Witts, J.D., Newton, R.J., Mills, B.J.W., Wignall, P.B., Bottrell, S.H., Hall, J.L.O., Francis, J.E., and Alistair Crame, J., 2018, The impact of the Cretaceous-Paleogene (K-Pg) mass extinction event on the global sulfur cycle: Evidence from Seymour Island, Antarctica: *Geochimica et Cosmochimica Acta*, v. 230, p. 17–45, <https://doi.org/10.1016/j.gca.2018.02.037>.
- Zachos, J., and Arthur, M., 1986, Paleoceanography of the Cretaceous/Tertiary boundary event: Inferences from stable isotopic and other data: *Palaeogeography and Palaeoclimatology*, v. 1, p. 5–26, <https://doi.org/10.1029/PA001i001p00005>.

Printed in USA